

Shorter contribution

The contribution of locally generated MTSat-1R atmospheric motion vectors to operational meteorology in the Australian region

J. Le Marshall^{1,2}, R. Seecamp¹, M. Dunn², C. Velden³, S. Wanzong³, K. Puri¹,
R. Bowen¹ and A. Rea¹

¹Centre for Australian Weather and Climate Research – A partnership between the Australian Bureau of Meteorology and CSIRO, Australia

²Physics Department, Latrobe University, Australia

³CIMSS, University of Wisconsin, USA

Introduction

The Multi-functional Transport Satellite – 1 Replacement (MTSat-1R) was launched on 26 February 2005. It was subsequently moved over the equator to 140°E where it has been operated by the Japanese Meteorological Agency (JMA) as the primary geostationary meteorological satellite, observing the Western Pacific, Asia and the Australian region. Since 2005, MTSat-1R data have been received at the Bureau of Meteorology (hereafter referred to as ‘the Bureau’) satellite groundstation at Crib Point (38.3°S, 145.2°E) Victoria, and calibrated and navigated radiance data (imagery) have been used to calculate atmospheric motion vectors (AMVs). The AMVs have been error characterised and used in real-time trials to gauge their impact on operational regional numerical weather prediction (NWP). Their benefit is described below. They are used, operationally, for analysis in the Darwin Regional Forecasting Centre (RFC) and, after these trials, were introduced into the Bureau’s National Meteorological and Oceanographic Centre’s (NMOC’s) operational NWP suite with the upgrade of the operational regional prediction system in October 2007.

Background

Australia’s position in the data-sparse southern oceans has resulted in dependence on satellite remote sensing for high-quality analysis and NWP in our region.

AMVs make an important contribution to the satellite database, being, for example, one of the most important satellite observations for tropical cyclone track prediction. To provide accurate and timely winds for operational NWP in the Australian region, AMVs have been calculated locally, from sequential GMS images (Le Marshall et al. 1994, 2002), GOES-9 images (Le Marshall et al. 2004b), and now MTSat-1R images. These have been used to provide AMVs at 15-minute intervals, four times daily, and hourly for the rest of the time. Winds have been generated using infrared (11 µm), visible (0.5 µm) and water vapour absorption (6.7 µm) band images. Here we examine the generation, quality control and application of winds generated from triplets of 15-minute interval infrared imagery every six hours. In the future, the hourly generation of winds will allow their use in four-dimensional variational assimilation (4D Var), where their utility for tropical cyclone prediction has already been demonstrated (Le Marshall et al. 1996, 2000a; Leslie et al. 1998).

The methods used at the Bureau in the past to estimate AMVs, from GMS-5 VISSR data, are largely covered in Le Marshall et al. (1999, 2000b). Sequential infrared (IR), visible (VIS) or water vapour (WV) band images (a triplet), usually separated by an hour or half an hour, were used for velocity estimation. As a result, high density winds were generated continuously at hourly or half-hourly intervals. Selected targets in the imagery were tracked automatically using a lagged correlation technique, which minimised root mean square (RMS) differences in brightness from successive pictures to estimate the vector displacement. Cloud-height assignment used forecast temper-

Corresponding author address: J.F. Le Marshall, Centre for Australian Weather and Climate Research, GPO Box 1289, Melbourne, 3001, Australia.
Email: j.lemarshall@bom.gov.au

ature profiles. The cloud height assigned for low-level clouds was that of the cloud base (following the work of Hasler et al. (1976, 1977)). The benefit of cloud-base height assignment is shown in Le Marshall and Pescod (1994). Height assignment involved fitting Hermite polynomials to smooth raw histograms of brightness temperature, enabling estimation of cloud-base altitude from cloud-base temperature. Upper-level AMVs were assigned to the cloud-top altitude which was estimated using 11 and 12 μm split window observations (Le Marshall et al. 1998). For water vapour AMVs, height assignment of the upper and middle-level AMVs in clear conditions was described in Le Marshall et al. (1999). Error characteristics of the AMVs were also determined and each vector was assigned several error indicators, including the expected error (EE) and quality indicator (QI). The associated correlated error and length scale (Le Marshall et al. 2004a) were also provided.

When the GOES-9 satellite replaced GMS-5 in 2003, methods similar to those employed at NESDIS (Daniels et al. 2000) and also at the Bureau (Le Marshall et al. 2000b) were used to generate AMVs from GOES-9 GVAR data received at the Bureau's groundstation at Crib Point (Le Marshall et al. 2004b). In this system, target selection began with a search for tracers using bidirectional brightness temperature gradients in 15 x 15 pixel boxes. Gradients were examined to ensure that cloud edges were being tracked and prospective targets were subjected to a spatial coherence analysis (Coakley and Bretherton 1982) and tracked using a lagged correlation technique. After tracer selection, three sequential GOES-9 infrared images were carefully navigated using matching of land features to ensure that there was consistency between the images used for estimating cloud displacement. The height assignment method used for upper-level AMVs was based on Schmets et al. (1993). The technique employed was the H_2O -intercept method, using 11 μm (channel 4) observations and the 6.7 μm (channel 3) observations. Radiances from the IR and WV channels were measured and compared to calculate Planck blackbody radiances as a function of cloud-top pressure. The cloud-top altitude was then inferred from a linear extrapolation of radiances onto the calculated curve of opaque cloud radiances, providing the target altitude. The approach was described in Nieman et al. (1993). The low-level AMV altitude assignment technique was similar to that developed in the Bureau (Le Marshall et al. 2000b) where cloud altitude was assigned to the cloud base for low-level vectors. As with the GMS-5, the error characteristics of these vectors were determined and each vector was associated with error indicators such as the EE and QI as well as with a correlated error and length scale.

MTSat-1R atmospheric motion vectors

When MTSat-1R replaced GOES-9 in 2005, again, methods similar to those employed at NESDIS (Daniels et al. 2000, Velden et al. 2005) and also at the Bureau (Le Marshall et al. 2000b) were used to generate AMVs from the MTSat-1R HIRID data received at the Crib Point groundstation. Three sequential images from MTSat-1R were navigated using land features to ensure that there was consistency between images used for estimating cloud displacement. In this system, target selection for IR (11 μm) targets commenced with a search for tracers, using bidirectional brightness temperature gradients in 15 x 15 pixel boxes. As in the case of GOES-9, targets with gradient features were subjected to a spatial coherence analysis (Coakley and Bretherton, 1982) and tracked using lagged correlation. Height assignment methods were similar to those employed for GOES-9. Figure 1(a) is an example of the local MTSat-1R IR AMVs generated for 1200 UTC on 18 March 2007. Figure 1(b) shows typical operational usage of local and JMA MTSAT-1R AMVs. The schedule for generating these MTSat-1R based winds can be seen in Table 1.

Accuracy and quality control

Careful quality control (QC) and error characterisation ensure the AMVs have a beneficial impact on NWP (Le Marshall et al. 2004a). Error characterisation used the Bureau's initial error flag (ERR), which involved a number of basic checks (first guess departure check, vector pair acceleration check, tracer constancy check etc.), the QI (Holmlund et al. 1998), and the more recent EE (Le Marshall et al. 2004a).

These error indicators are used to effectively thin the AMVs and to ensure good data coverage with average separations consistent with the length scale of the correlated error. The thinning methodology has also ensured that the errors are usually less than the background error field of the forecast model measured at radiosonde sites. The approach is detailed in Le Marshall et al. (1994). The EE now has several components, the total root mean square (rms) error (m/s) currently used operationally, the meridional and the zonal error components (m/s), the vector height error (hPa) and the wind vector determination error (m/s), often due to navigation and tracking related inaccuracies. The total rms error component of the EE has been used in this study. It has also been placed in the BUFR code used by other systems (e.g. at NOAA/ NESDIS) as the quality indicator, QI(EE), where

$$QI(EE) = (100 - 10.0 * EE) \quad \dots 1$$

Fig. 1(a) MTSat-1R IR1 AMVs generated around 1200 UTC on 18 March 2007. Magenta denotes upper level tropospheric vectors, yellow, lower level tropospheric vector.

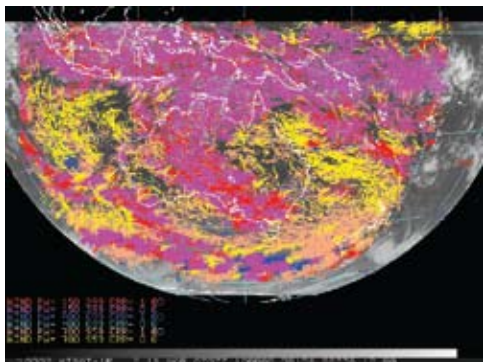
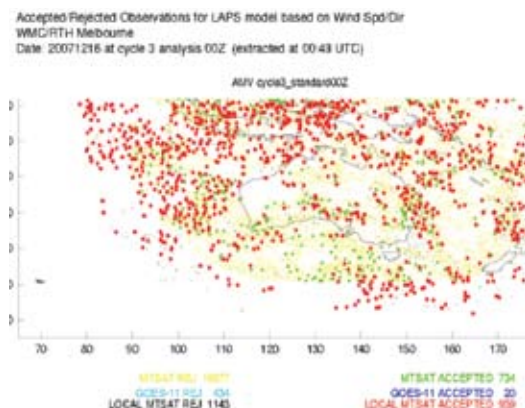


Fig. 1(b) MTSat-1R AMVs used in the operational analysis at the Bureau of Meteorology at 0000 UTC on 16 December 2007. Red denotes local vectors, green vectors are from JMA.



A typical comparison of the EE with the actual error for MTSat-1R IR winds is seen in Fig. 2. Here, the rms error component of the EE has been compared to the actual rms error determined using contemporaneous radiosonde data within 150 km of the AMVs and is seen to be an effective tool for selecting high-quality AMVs.

Fig. 2(a) Measured error (m/s) versus EE for high-level MTSAT-1R IR winds (13 March–12 April 2007).

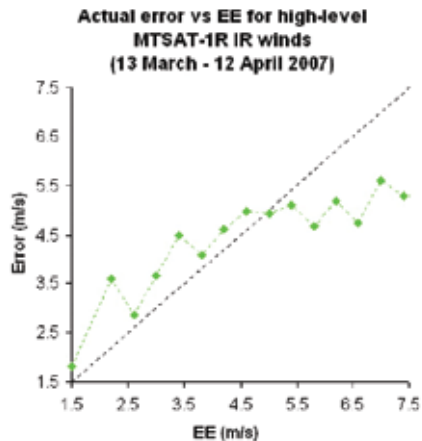
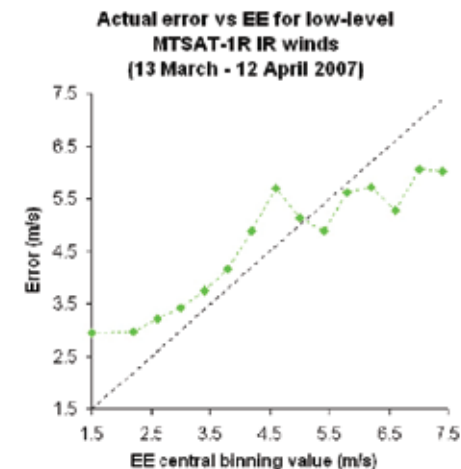


Fig. 2(b) Measured error (m/s) versus EE for low-level MTSAT-1R IR winds (13 March–12 April 2007).



Quality control of AMVs to provide low, middle and high-level data in the Bureau system has used all three error indicators (EE, QI, ERR). Typical accuracy of the AMVs available for NWP is given in Table 2 which shows the mean magnitude of vector difference (MMVD) between MTSat-1R AMVs and radiosondes winds within 150 km in the Australian region for March 2007.

Table 1. Real-time schedule for MTSat-1R AMVs at the Bureau of Meteorology. Sub-satellite image resolution, frequency and time of wind extraction and separations of the image triplets used for wind generation are indicated.

Wind type	Resolution	Frequency-times (UTC)	Image separation
Real time IR	4 km	Six-hourly – 00, 06, 12, 18	15 minutes
Real time IR (hourly)	4 km	Hourly – 00, 01, 02, 03, 04, 05, . . . , 23	1 hour

Table 2. Mean magnitude of vector difference (MMVD) between MTSat-1R AMVs, forecast model first guess and radiosonde winds within 150 km for March 2007.

Level	No. of observations	First guess MMVD ($m s^{-1}$)	AMV
MMVD ($m s^{-1}$)			
Low 950 – 700 hPa	192	2.67	2.92
Middle 699 – 400 hPa	88	3.79	3.75
High 399 – 150 hPa	706	4.13	4.08

Correlated error

As with earlier geostationary satellite local AMV systems, the correlated error has been analysed for the Bureau produced MTSat-1R winds (Le Marshall et al. 2004a). The correlated error and its spatial variation (length scale) were determined using the second-order auto regressive (SOAR) function

$$R(r) = R_0 + R_0(1 + r/L) \exp(-r/L) \dots 2$$

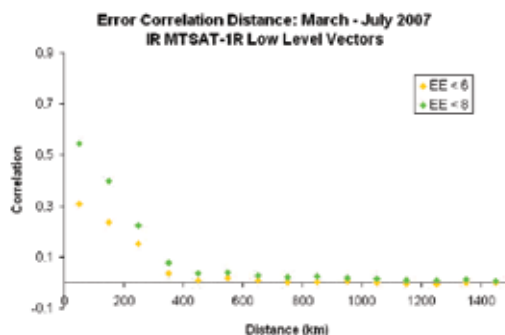
where $R(r)$ is the error correlation, R_0 and R_{00} are the fitting parameters (greater than 0), L is the length scale and r is the separation of the correlates. Thus, the difference between AMV and radiosonde winds (error) has been separated into correlated and non-correlated parts. A typical variation of error correlation with distance for MTSat-1R IR1 AMVs is seen in Fig. 3, while the parameters of the SOAR function which best fits the observations are in Table 3.

These length scales may be compared to those from GMS-5, namely, 123 km and 73 km, for low and high-levels respectively, where the GMS-5 vectors were subjected to a quality control regime close to that of $EE < 6$.

Real-time assimilation trials

Before local MTSat-1R data could be incorporated into the Bureau's operational NWP suite, real time assimilation trials using MTSat-1R infrared channel 1 (IR1) AMVs were undertaken using the then current operational limited area prediction system (LAPS) of March 2007 configured to run at 0.375° horizontal resolution with 51 levels in the vertical. The system and methodology are described below. A trial was also conducted using the Bureau's next (October 2007) operational LAPS system which includes 61 vertical levels and 0.375° resolution. The results from both tests were similar and consistent with earlier results from assimilation of GMS-5 and GOES-9 local vectors (e.g. Le Marshall et al. 2002; Le Marshall et al. 2004b).

Fig. 3 Error correlation versus distance (100 km bins) for low level MTSat 1R AMVs with $EE < 6$ and $8 m/s$ (March – July 2007).



The assimilation system

The assimilation methodology employed the real time operational NMOC regional LAPS, using all available data (including all available JMA AMVs) as the control. The analyses on which the forecasts reported here are based start with a Bureau global analysis and prognosis system (GASP) global analysis (Seaman et al. 1995), valid 12 hours prior to the forecast start time. This is used as a first guess to the regional analysis which then provides the base analysis for an initialised six-hour forecast, a subsequent analysis and a further initialised six-hour forecast. This forecast is then used as a first guess to the final analysis from which the 24 and 48-hour forecasts are run. Forecasts are nested in fields from the most recent GASP forecast (Bourke et al. 1995).

The analysis and forecast models

The LAPS analysis and forecast model uses a common latitude/longitude/sigma coordinate system. The configuration consisted of 320×220 grid-points at 0.375° spacing in the horizontal, and 51 levels (L51) in the vertical, with an upper level of sigma 0.01. A

Table 3. Parameters of the SOAR function (Eqn 2) which best model the measured error correlations for the MTSat-1R AMVs listed in the left column. (February – April, 2007).

<i>MTSat-1R IR1 AMVS</i>	<i>R00</i>		<i>RO</i>		<i>L (km)</i>	
	<i>Low</i>	<i>High</i>	<i>Low</i>	<i>High</i>	<i>Low</i>	<i>High</i>
EE < 6	0.006	0.370	0.460	0.460	86.000	99.900
EE < 8	0.066	0.052	0.640	0.440	122.700	110.900

second version of the LAPS with 61 levels (L61) in the vertical and an upper sigma level of 0.0001 was also used in these tests. The analysis system was a limited area adaptation of the global multivariate statistical interpolation analysis (Seaman et al. 1995). The errors assigned to the atmospheric motion vectors in the operational analysis scheme are 3 m s⁻¹, 4 m s⁻¹ and 5 m s⁻¹ for low, middle and high-level vectors respectively. These numbers are consistent with the errors of 3 m s⁻¹ assigned to local middle and high-level radiosonde observations and the differences between collocated local AMVs and radiosonde wind estimates usually recorded at the Bureau.

The forecast model is described in Puri et al. (1998) and is a hydrostatic model formulated in latitude/longitude/sigma coordinates on the Arakawa A grid. It uses high-order numerics and includes a comprehensive physics package and the digital filter initialisation of Lynch and Huang (1992).

Method

In the real-time trial MTSAT 1R AMVs generated using 11 μm (Channel IR1) and 6.7 μm (Channel IR3) imagery were added to the operational regional assimilation system. The operational regional NWP system already contains AMVs from the JMA, available up to the operational cut off time (analysis time + 1.75 hours; 0.75 hours when daylight saving applies), which may preclude on time vectors. The methodology was similar to that used in Le Marshall et al. (2002). The accuracy of the real time AMVs provided to the assimilation system for the period studied in the first experiment with L51 LAPS in mid 2007 is summarised in Table 4 which shows the MMVD and RMS difference between AMVs and radiosondes within 150 km, and, in the case of low level vectors between AMVs and radiosonde at 150 km and also at 30 km separation. It can be seen that, the accuracy of the local AMVs at radiosonde sites is better than that of the forecast model first guess field used when calculating the winds, although, for low-level vectors, a more stringent collocation criterion between the AMVs and the radiosondes for calculating errors was required for this to be the case. In this study, local quality-control

methods were used to provide vectors with expected error consistent with the error levels anticipated for AMVs in the operational analysis. The data used for this operational trial were generated from triplets of IR and WV images centred at 0000, 0600, 1200 and 1800 UTC where the images used were separated by 15 minutes. The system provided AMV coverage and accuracy consistent with the correlated error length scale and expected error, and the resolution characteristics of the data and data assimilation system.

A series of parallel real-time forecasts was run using the operational forecast system with AMV data added to the operational database, which included all available MTSat 1R AMVs from JMA. The experimental period was from 0000 UTC 30 May to 1200 UTC 15 June 2007 (34 cases). The experimental period was relatively short but encompassed a variety of synoptic patterns in the Australian region, including blocking sequences in the Tasman Sea. For these real-time forecasts, the S1 skill scores (Teweles and Wobus 1954) were calculated on the NMOC operational verification grid using 0000 UTC and 1200 UTC analyses. The verification grid consists of 58 points within the domain 90° E to 170° E, 15° S to 55° S. The exact grid is seen in Bennett and Leslie (1981).

A test was also conducted for the period 1 September to 8 October 2007 (72 cases), using the next (now current) operational version of LAPS. The significant changes to LAPS with this implementation are an extension to 61 levels (L61) in the vertical and the reinstatement of local direct readout ATOVS.

Results

The S1 skill scores for 24-hour forecasts from using MTSAT 1R AMV data in the May 2007 operational (L51) LAPS model are compared to the operational skill scores in Table 5(a). The statistics are consistent with those recorded in earlier impact studies with GMS-5 (Le Marshall et al. 2002) and GOES-9 (Le Marshall et al. 2004) where a modest positive impact, mainly in the lower levels, was recorded. The S1 skill scores for the new L61 LAPS (72 cases) are shown

Table 4. Mean magnitude of vector difference (MMVD) and root mean square difference (RMSD) between MTSat 1R AMVs, forecast model first-guess winds and radiosonde winds for the period 30 May to 15 June 2007.

<i>Level</i>	<i>Data source</i>	<i>Bias (m s⁻¹)</i>	<i>No. of obs</i>	<i>MMVD (m s⁻¹)</i>	<i>RMSD (m s⁻¹)</i>
High – up to 150 km separation between radiosondes and AMVs	AMVs	-0.55	1386	3.90	4.47
	First Guess	1.3776	1386	4.42	5.09
Low - up to 150 km separation between radiosondes and AMVs	AMVs	-0.76	540	3.18	3.72
	First Guess	-0.70	540	2.72	3.12
Low – up to 30 km separation between radiosondes and AMVs	AMVs	-0.44	18	2.45	3.08
	First Guess	-0.20	18	2.67	3.07

Table 5(a). 24-hour forecast verification S1 skill score for the May 2007 operational regional forecast system (L51 LAPS) and L51 LAPS with IR, six-hourly image based AMVs for 30 May to 15 June 2007 (34 cases).

<i>Level</i>	<i>(LAPS) S1</i>	<i>(LAPS + MTSAT-IR AMVs) S1</i>
MSLP	19.00	18.81
1000 hPa	21.35	20.80
900 hPa	22.42	22.08
850 hPa	22.81	22.76
500 hPa	15.96	15.91
300 hPa	13.65	13.65
250 hPa	12.62	12.58

Table 5(b). 24-hour forecast verification S1 skill score for the next operational regional forecast system (L61 LAPS) and L61 LAPS with IR, six-hourly image-based AMVs for 1 September to 8 October 2007 (72 cases).

<i>Level</i>	<i>(LAPS) S1</i>	<i>(LAPS + MTSAT-IR AMVs) S1</i>
MSLP	20.24	19.15
1000 hPa	20.06	19.13
900 hPa	18.65	17.75
850 hPa	17.41	16.69
500 hPa	12.41	11.73
300 hPa	10.49	9.76
250 hPa	12.41	11.90

in Table 5(b). A positive impact consistent with previous results for local GMS-5 and GOES-9 AMVs was again recorded. The results show that real time MTSAT 1R IR and WV image based AMVs, are of an accuracy which can benefit operational NWP in the Australian region. Addition of the vectors to the operational regional forecast system which already contains some JMA AMVs, has provided both improved data coverage of the region and a small average forecast improvement. The results and their consistency with previous studies has led to a reintroduction of these local AMVs into operational use.

Summary and conclusions

The local estimation of real time operational MTSAT 1R AMVs and their impact on operational regional

NWP has been described. Experiments using these data in a real time NWP trial have been summarized. Their benefit to current operational regional NWP, when used with a control employing NMOC's full operational data base (including JMA AMVs), has been recorded. These results were consistent with past trials with GMS-5 and GOES-9 and have resulted in a reintroduction of local vectors into operations.

This trial has been followed by new studies of the impact of 6-hourly visible image based AMVs and hourly AMVs in the current operational systems and a study of the use of continuous (at least hourly) AMVs in the next generation 4-D VAR United Kingdom Meteorological Office Unified Model based system.

Looking ahead, the continuing trend to space based observations with higher spatial, temporal and spectral resolution should enable improved estimation of atmospheric motion and result in quantitative benefit to

NWP. In the near future, the prospects of benefits from the expanded use of sequential observations from MTSat 2 and the Chinese satellite, FY 2 and also from next generation ultraspectral instruments such as the geostationary imaging Fourier transform spectrometer (GIFTS) (Smith et al. 2000) are very good.

Acknowledgments

Thanks are due to Bert Berzins, Ian Senior and Weiqing Qu for assistance in data access and to Terry Adair for assistance in the preparation of this manuscript.

References

- Bennett, A.F. and Leslie, L.M. 1981. Statistical Correction of the Australian Region Primitive Equation Model. *Mon. Weath. Rev.*, 109, 453-62.
- Bourke, W.P., Hart, T., Steinle, P., Seaman, R., Embery, G., Naughton, M. and Rikus, L. 1995. Evolution of the Bureau of Meteorology's Global Assimilation and Prediction System. Part 2: Resolution enhancements and case studies. *Aust. Met. Mag.*, 44, 19-40.
- Coakley, J. and Bretherton, F. 1982. Cloud cover from high resolution scanner data: Detecting and allowing for partially filled fields of view. *J. Geophys. Res.*, 87, 4917-32.
- Daniels, J., Velden, C., Busby, W. and Irving, A. 2000. Status and Development of Operational GOES Wind Products. *Proc. Fifth International Winds Workshop*, Lorne, Australia, 28 – 31 March 2000. Published by EUMETSAT EUM P28 ISSN 1023-0414, 27-45.
- Hasler, A. F., Shenk, W. and Skillman, W. 1976. Wind estimates from cloud motions: Phase I of an in situ aircraft verification experiment. *Jnl appl. Met.*, 15, 10-15.
- Hasler, A.F., Shenk, W. and Skillman, W. 1977. Wind estimates from cloud motions: preliminary results of phase I, II and III of an in situ aircraft verification experiment. *Jnl appl. Met.*, 16, 812-5.
- Holmlund, K. 1998. The utilization of statistical properties of satellite-derived atmospheric motion vectors to derive quality indicators. *Weath. forecasting*, 13, 1093-104.
- Le Marshall, J.F., Pescod, N., Seaman, R., Mills, G. and Stewart, P. 1994. An Operational System for Generating Cloud Drift Winds in the Australian Region and Their Impact on Numerical Weather Prediction. *Weath. forecasting*, 9, 361-70.
- Le Marshall, J.F. and Pescod, N. 1994. Generation and application of cloud drift winds in the Australian Region - recent advances. *Proceedings of the Pacific Ocean Remote Sensing Conference*, Melbourne, Australia, 1 - 4 March, 1994, 467-74.
- Le Marshall, J.F., Leslie, L.M. and Bennett, A.F. 1996. Tropical cyclone Beti - an example of the benefits of assimilating hourly satellite wind data. *Aust. Met. Mag.*, 45, 275-84.
- Le Marshall, J.F., Pescod, N., Seecamp, R., Spinoso, C. and Rea, A. 1998. Improved Weather Forecasts from Continuous Generation and Assimilation of High Spatial and Temporal Resolution Winds. *Proc. Fourth International Winds Workshop*, Saanenmoser, Switzerland, 20-24 October, 1998, 101-8.
- Le Marshall, J.F., Pescod, N., Seecamp, R., Puri, K., Spinoso, C. and Bowen, R. 1999. Local estimation of GMS-5 water vapour motion vectors and their application to Australian region numerical weather prediction. *Aust. Met. Mag.*, 48, 73-77.
- Le Marshall, J., Leslie, L., Morison, R., Pescod, N., Seecamp, R. and Spinoso, C. 2000a. Recent Developments in the Continuous Assimilation of Satellite Wind Data for Tropical Cyclone Track Forecasting. *Adv. Space Res.*, 25, 1077-80.
- Le Marshall, J.F., Pescod, N., Seecamp, R., Rea, A., Tingwell, C., Ellis, G. and Shi, H. 2000b. Recent Advances in the quantitative generation and assimilation of high spatial and temporal resolution satellite winds. *Proc. Fifth International Winds Workshop*, Lorne, Australia, 28 – 31 March 2000. Published by EUMETSAT EUM P28 ISSN 1023-0414. 47-56.
- Le Marshall, J., Mills, G., Pescod, N., Seecamp, R., Puri, K., Stewart, P., Leslie, L.M. and Rea, A. 2002. The estimation of high density atmospheric motion vectors and their application to operational numerical weather prediction. *Aust. Met. Mag.*, 51, 173 -80.
- Le Marshall, J., Rea, A., Leslie, L., Seecamp, R. and Dunn, M. 2004a. Error Characterization of Atmospheric Motion Vectors. *Aust. Met. Mag.*, 53, 123-31.
- Le Marshall, J., Seecamp, R., Daniels, J., Velden, C., Puri, K., Bowen, R., Rea, A., Dunn, M. 2004b. The contribution of GOES-9 to operational NWP forecast skill in the Australian region. *Aust. Met. Mag.*, 53, 279-83.
- Leslie, L.M., Le Marshall, J. F., Morison, R. P., Spinoso, C., Purser, R. J. Pescod, N. and Seecamp, R. 1998. Improved Hurricane Track Forecasting from the Continuous Assimilation of High Quality Satellite Wind Data. *Mon. Weath. Rev.*, 126, 1248-58.
- Lynch, P and Huang, X-Y. 1992. Initialization of the HIRLAM Model using a digital filter. *Mon. Weath. Rev.*, 120, 1019-34.
- Nieman, S., Schmetz, J. and Menzel, W.P. 1993. A comparison of several techniques to assign heights to cloud tracers. *Jnl appl. Met.*, 32, 1559-68.
- Puri, K., Dietachmeyer, G.S., Mills, G.A., Davidson, N.E., Bowen, R.M. and Logan L.W. 1998. The new BMRC Limited Area Prediction System. *LAPS. Aust. Met. Mag.*, 47, 203-23.
- Schmetz, J., Holmlund, K., Hoffman, J., Strauss, B., Mason, B., Gaertner, V., Koch, A. and Van Der Berg, L. 1993. Operational cloud motion winds from METEOSAT infrared images. *Jnl appl. Met.*, 32, 1206-55.
- Seaman, R., Bourke, W., Steinle, P., Hart, T., Embery, G., Naughton, M. and Rikus, L. 1995. Evolution of the Bureau of Meteorology's Global Assimilation and Prediction system. Part 1: analysis and initialisation. *Aust. Met. Mag.*, 44, 1-18.
- Smith, W.L., Harrison, F.W., Revercomb, H.E., Bingham, G.E., Huang H.L. and Le Marshall, J.F. 2000. The Geostationary Imaging Fourier Transform Spectrometer. *Proc. Eleventh International TOVS Study Conference*, Budapest, Hungary. 391-398.
- Teweles, S. and Wobus, H. 1954. Verification of Prognostic Charts. *Bull. Am. Met. Soc.*, 35, 455-63.
- Velden, C., Daniels, J., Stettner, D., Santek, D., Key, J., Dunion, J., Holmlund, K., Dengel, G., Bresky, W. and Menzel, P. 2005. Recent innovations in deriving tropospheric winds from meteorological satellites. *Bull. Am. Met. Soc.*, 86, 205-23.